

Enhanced photocurrent and conversion efficiency in thin-film microcrystalline silicon solar cells using periodically textured back reflectors with hexagonal dimple arrays

Hitoshi Sai, Kimihiko Saito, and Michio Kondo

Citation: *Appl. Phys. Lett.* **101**, 173901 (2012); doi: 10.1063/1.4761956

View online: <http://dx.doi.org/10.1063/1.4761956>

View Table of Contents: <http://apl.aip.org/resource/1/APPLAB/v101/i17>

Published by the American Institute of Physics.

Additional information on Appl. Phys. Lett.



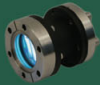



Journal Homepage: <http://apl.aip.org/>

Journal Information: http://apl.aip.org/about/about_the_journal

Top downloads: http://apl.aip.org/features/most_downloaded

Information for Authors: <http://apl.aip.org/authors>

ADVERTISEMENT

a sampling of our products		for surface and materials science	www. rbdinstruments .com	celebrating over 20 years of innovation
 deposition tools	 desorption systems	 sputter ion sources	 viewports	 usb picoammeters

Enhanced photocurrent and conversion efficiency in thin-film microcrystalline silicon solar cells using periodically textured back reflectors with hexagonal dimple arrays

Hitoshi Sai (齋均),^{1,a)} Kimihiko Saito (齊藤公彦),² and Michio Kondo (近藤道雄)¹

¹Research Center for Photovoltaic Technologies, National Institute of Advanced Industrial Science and Technology (AIST), Central 2, Umezono 1-1-1, Tsukuba, Ibaraki 305-8568, Japan

²Photovoltaic Power Generation Technology Research Association (PVTEC), Tsukuba 305-8568, Japan

(Received 3 September 2012; accepted 8 October 2012; published online 22 October 2012)

Periodically textured back reflectors with hexagonal dimple arrays are applied to thin-film microcrystalline silicon ($\mu\text{c-Si:H}$) solar cells for enhancing their photon absorption and photovoltaic performance. In a systematic survey of 1- μm -thick $\mu\text{c-Si:H}$ cells, the best performance is obtained with a period of 1.5 μm and an aspect ratio of 0.20–0.25 with a high current density exceeding 26 mA/cm^2 and a marked efficiency of 10.1%. These results demonstrate the high potential of periodic textures or surface gratings for improving the conversion efficiency of thin-film silicon solar cells. © 2012 American Institute of Physics. [<http://dx.doi.org/10.1063/1.4761956>]

Thin-film silicon solar cells (TFSSCs) form a promising candidate for future large-area photovoltaic systems operating in the gigawatt range because of the abundance and non-toxicity of the source materials.^{1,2} In TFSSCs, the use of the so-called light trapping technology is important for absorbing photons within thin Si films owing to their insufficient carrier transport properties or film deposition cost. Using a thin hydrogenated amorphous Si (a-Si:H) active layer is also advantageous for mitigating the well-known light-induced degradation effect.³ For this purpose, textured substrates have been implemented to scatter the incident light and elongate the optical path length inside the cells.^{1,2,4–23} In an ideal case, the optical path length in TFSSCs can be enhanced by a factor of $4n^2$, where n is the refractive index of thin-film Si.²⁴

In the recent years, periodically textured substrates or surface gratings have been actively studied as a more sophisticated platform with the potential for achieving higher current density than conventional random textures.^{8–23} Recently, Battaglia *et al.* demonstrated that when an optimized periodic texture is applied to a-Si:H solar cells, it improves the conversion efficiency as well as the current density at the same level as state-of-the-art random textures.⁸ Application of periodic textures to $\mu\text{c-Si:H}$ solar cells, in which more efficient light confinement is necessary, owing to their very small absorption coefficient in the infrared (IR) region, has also been intensively studied both experimentally and theoretically.^{13–21} However, the potential of using periodic textures in $\mu\text{c-Si:H}$ cells, not only for higher current but also higher efficiency, has not yet been demonstrated experimentally. It is well known that excessively steep textures such as binary surface-relief gratings or pyramidal textures with V-shaped valleys often induce defects in $\mu\text{c-Si:H}$ films and impair photovoltaic performance.²⁵ Hence, it is vital to use appropriate textures that are suitable for high-quality film growth as well as good light

confinement. Recently, we reported that periodically textured substrates with hexagonal dimple arrays (hereafter referred to as the “honeycomb texture”) have the potential to improve photon absorption and conversion efficiency in $\mu\text{c-Si:H}$ cells.¹⁶ In this Letter, we report that carefully chosen honeycomb textures result a high current density of more than 26 mA/cm^2 and a conversion efficiency exceeding 10% in n - i - p $\mu\text{c-Si:H}$ solar cells with a thickness of only 1 μm . We also show, by a systematic survey, that there is a preferable period and aspect ratio of periodic textures that can be used to achieve this high performance.

Honeycomb textures were fabricated by the following procedure: A hexagonal photo-resist pattern was formed on a Si wafer with a thermally grown SiO_2 film using photolithography. Next, the wafer was soaked in a diluted buffered hydrofluoric acid (BHF) solution to transfer the hexagonal pattern onto the SiO_2 film. After removing the remaining resist, a Ag/ZnO:Ga stacked film (200 nm/100 nm) was deposited onto the honeycomb-textured SiO_2 layer by sputtering to obtain a highly reflective and conductive surface.

Substrate-type n - i - p $\mu\text{c-Si:H}$ cells with an active area of 1 cm^2 were fabricated on these substrates. The structure of the solar cells consisted of a honeycomb-textured substrate/Ag/ZnO/ $\mu\text{c-Si:H}$ n - i - p layers/ In_2O_3 :Sn (ITO, 70 nm)/Ag grid. The intrinsic $\mu\text{c-Si:H}$ layer was deposited with conventional plasma-enhanced chemical vapor deposition (PECVD) using a SiH_4/H_2 gas mixture. Throughout this study, the thickness of the $\mu\text{c-Si:H}$ i layers was maintained at 1 μm . n - and p -type $\mu\text{c-Si:H}$ were also deposited by PECVD using PH_3 and B_2H_6 as dopant gases, respectively. For some solar cells, wide-gap p -type nc- SiO_x :H was also applied to reduce the absorption loss in the p -layer. The top ITO film and Ag finger-grid electrodes were deposited by sputtering at room temperature. Isolation of the cells was done by reactive ion etching. Finally, all the cells were annealed at 175 °C for 2 h. The performance of the cells was evaluated by measuring current density-voltage (J - V) characteristics with a dual-light solar simulator under AM 1.5 G 100 mW/cm^2 , and external quantum efficiency (EQE) spectra. Reflectivity of the cells

^{a)} Author to whom correspondence should be addressed. Electronic mail: hitoshi-sai@aist.go.jp.

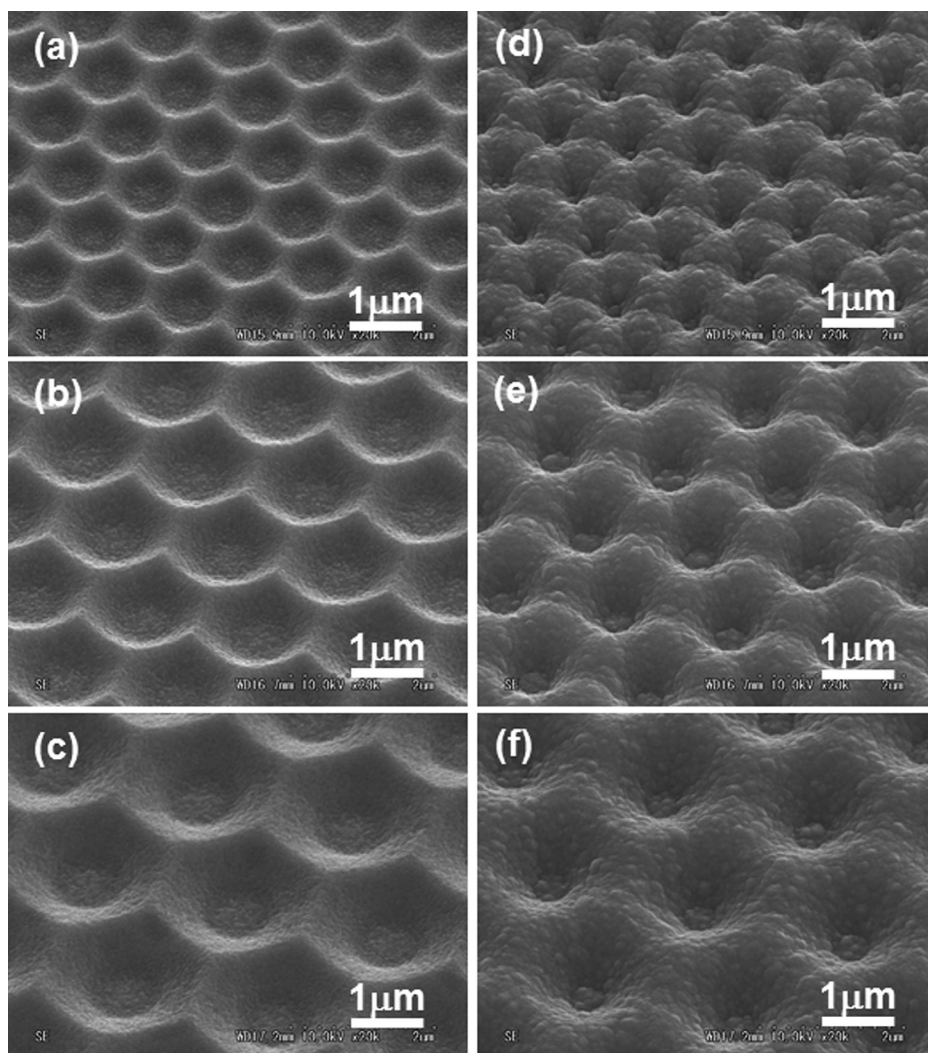


FIG. 1. (a)–(c) SEM images of 3 different periodic honeycomb textures and (d)–(f) the surfaces of the 1- μm -thick $\mu\text{c-Si:H}$ solar cells deposited on them. The periods of the substrates are (a) and (d) 1 μm , (b) and (e) 1.5 μm , and (c) and (f) 2 μm .

was also investigated using a spectrometer with an integral sphere (Perkin Elmer, Lambda 950).

Uniform honeycomb textures were reproducibly obtained by using our fabrication procedure. Figures 1(a)–1(c) show scanning electron microscope (SEM) images of honeycomb-patterned substrates with 3 different periods: $P = 1.0 \mu\text{m}$, $1.5 \mu\text{m}$, and $2.0 \mu\text{m}$. All the substrates show a substantially uniform pattern regardless of the periods. The sides of the holes in each pattern can be tapered in a manner similar to a crater, as shown in Fig. 1, by properly utilizing the so-called undercut effect during BHF etching. Here, we define the aspect ratio in our honeycomb textures as the ratio of the peak height H to the period P , namely, H/P . The diameter of the flat area at the bottom of each dimple, D , can be controlled by modifying the photo-resist pattern and the etching condition. We use honeycomb textures with $0.3 < D/P < 0.5$ in this study. Figures 1(d)–1(f) show SEM images of the surface of 1- μm -thick $\mu\text{c-Si:H}$ cells deposited on the substrates shown in Figs. 1(a)–1(c). It was found that the morphology of the cell surfaces is not a simple replication of the substrate. The diameter of each dimple is reduced after $\mu\text{c-Si:H}$ film growth, and tiny holes are left behind on the cell surface, particularly for $P = 1 \mu\text{m}$.

The back reflectors with honeycomb textures are promising, owing to their potential for high conversion efficiency as well as high current density. In Fig. 2, J - V parameters of

the 1- μm -thick $\mu\text{c-Si:H}$ solar cells on the honeycomb textures with $P = 1.4$ and $1.5 \mu\text{m}$ are plotted as functions of H/P . As can be seen in Fig. 2(a), the short-circuit current density J_{SC} increases drastically with increasing H/P and

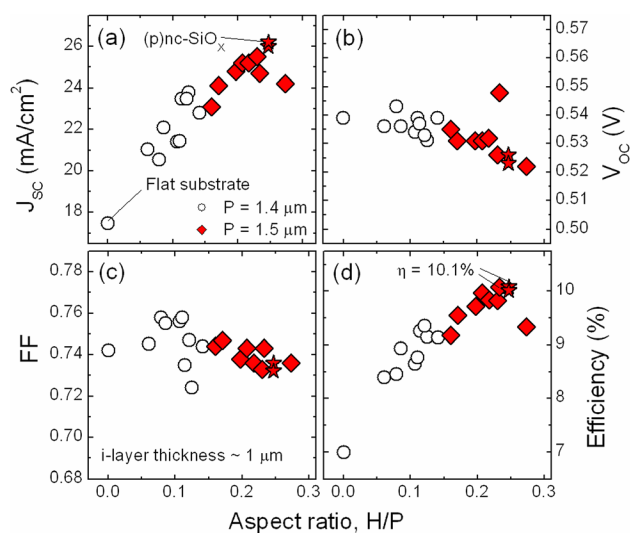


FIG. 2. J - V parameters of 1- μm -thick $\mu\text{c-Si:H}$ solar cells fabricated on honeycomb textures with periods of $P = 1.4 \mu\text{m}$ and $1.5 \mu\text{m}$ as functions of the aspect ratio, H/P . The star symbols represent the results obtained with a wide-gap $(p)\text{nc-SiO}_x$ layer instead of the standard $(p)\mu\text{c-Si:H}$ layer.

then saturates at $H/P \approx 0.25$. As maximum values, $J_{SC} = 25.5 \text{ mA/cm}^2$ and 26.2 mA/cm^2 were obtained for the cells with the standard $(p)\mu\text{c-Si:H}$ and $(p)\text{nc-SiO}_x\text{:H}$ layers, respectively. We believe that these are among the highest values reported thus far for thin $\mu\text{c-Si:H}$ cells with periodic textures. However, J_{SC} begins to decrease when H/P increases beyond a certain limit. Because the EQE spectrum was almost unchanged under negative bias voltages, this sample showed a sufficient collection of photo-generated carriers. In addition, it was found that the reflectivity of the honeycomb back reflectors decreases gradually when H/P increases, as is often observed in textured metal reflectors. Therefore, we ascribe this decrease in J_{SC} to the enhanced absorption loss within the cell that is mainly caused by the reduced reflectivity of the substrate with such a high H/P . The open-circuit voltage (V_{OC}) shows a slight decreasing trend against the variation in H/P , while the fill factor (FF) is rather stable, as plotted in Figs. 2(b) and 2(c). The decreasing trend in V_{OC} can be ascribed to the deterioration in the Si film quality due to the rougher growth surface and/or insufficient coverage by the doped layers. Overall, the cell performance is mainly governed by J_{SC} , and a markedly high efficiency of 10.1% is achieved at $H/P \approx 0.23$.

The period of honeycomb textures also has a significant effect on the J_{SC} in $\mu\text{c-Si:H}$ solar cells. Figure 3 shows the J_{SC} variation against the period of honeycomb textures up to $3 \mu\text{m}$ at high aspect ratios of more than 0.2. A series of data are plotted for the periods $1.4 \mu\text{m}$ and $1.5 \mu\text{m}$ to show the variation caused by changing H/P . In the range of $0 < P < 1 \mu\text{m}$, the J_{SC} obtained by utilizing quasi-periodically textured Al substrates fabricated by anodic oxidation¹⁴ are plotted as supplemental data. In these data, the aspect ratio is around 0.2 as well. It is clearly shown that the optimum period for realizing a high J_{SC} is around $1.5 \mu\text{m}$ in the case of $1\text{-}\mu\text{m}$ -thick cells, while a high J_{SC} of over 24 mA/cm^2 is achievable when P is in the range of $1\text{--}2 \mu\text{m}$. Recent theoretical considerations have shown that optimal light trapping occurs when the grating period approximately equals the material band edge, which is $\sim 1 \mu\text{m}$ in our case.^{22,23} This has been supported by several optical modeling results,^{17–19} although a slightly

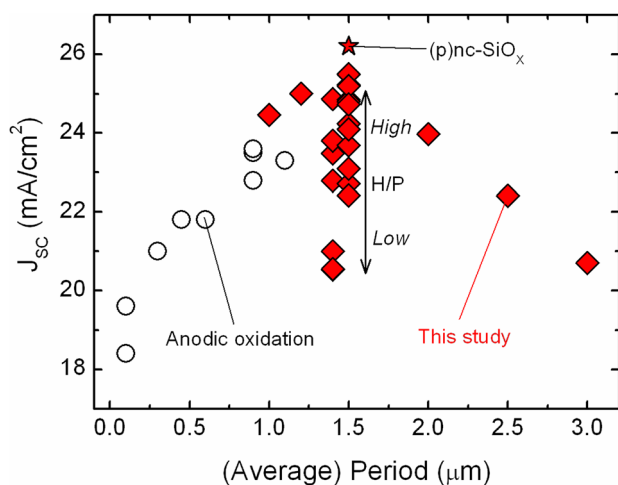


FIG. 3. Relationship between the period of textured substrates and the J_{SC} in $n\text{-i-p } \mu\text{c-Si:H}$ cells with a thickness of $1 \mu\text{m}$. Open circles represent data obtained with patterned Al substrates obtained by anodic oxidation of Al (see Ref. 14).

shorter period has been found to be optimal for binary gratings.^{17,20,21} However, we obtained the highest J_{SC} at a period of $1.5 \mu\text{m}$. We ascribe this discrepancy to the difference between the surface morphologies of the optical models and the devices. In optical modeling, an ideal texture is often assumed on both sides of the solar cells. However, in conventional TFSSCs, the morphology of the growth surface is not intentionally controlled, resulting in a complex morphology due to flattening and self-texturing during film growth. In fact, as seen in Figs. 1(d)–1(f), the dimples on the cell surface become smaller with a reducing period of the substrates, which results in a flatter cell surface and insufficient light trapping. To clarify this, we performed optical simulations based on finite-difference time domain (FDTD) and found that flattening the front surface of the cell reduces J_{SC} by several percent (not shown). In addition, an EQE enhancement by front texturing has been experimentally confirmed using $\mu\text{c-Si:H}$ cells with intentionally polished surfaces.¹⁴ In principle, the grating period should be larger than the cell thickness to avoid severe flattening of the cell surface. Therefore, in TFSSCs with an as-deposited surface morphology, the optimum period for light trapping is considered to be longer than that in ideal cell models according to their thickness.

Figure 4 shows the measured EQE spectra of the $1\text{-}\mu\text{m}$ -thick $\mu\text{c-Si:H}$ solar cells fabricated on flat and honeycomb-textured substrates. EQE in the wavelength range of $600\text{--}1100 \text{ nm}$ increases drastically upon applying the proper honeycomb texture with $P = 1.5 \mu\text{m}$ and $H/P > 0.2$, and this occurs on account of the enhanced light scattering and resulting improvement of light confinement in the device. The rough front surfaces, as shown in Fig. 1(e), contribute to the reduction in the primary reflection loss at the front interface across the entire wavelength region. In fact, a clear EQE improvement is also visible in the short wavelength region. As a consequence, a high current density of over 25 mA/cm^2 has been achieved using the conventional $(p)\mu\text{c-Si:H}$ layer. By replacing it with the wide-gap $(p)\text{nc-SiO}_x\text{:H}$ layer, the EQE can be further enhanced, mainly in the visible region, leading to a high current density of 26.2 mA/cm^2 . This is almost 50% higher than that of the reference flat cell.

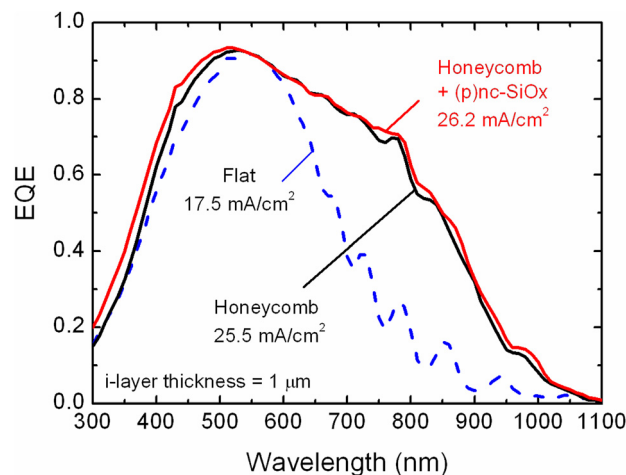


FIG. 4. External quantum efficiency spectra of the $\mu\text{c-Si:H}$ solar cells deposited on a flat substrate and a honeycomb texture with $P = 1.5 \mu\text{m}$ and an optimum H/P .

It is important to know the actual origins of such a remarkable enhancement in the EQE. Recently, Haug and his colleagues intensively studied the relationship between waveguide modes and light absorption enhancement in thin-film a-Si:H cells deposited on one-dimensional gratings.^{9–11} They demonstrated that the EQE (or absorption) peaks at specific wavelengths correspond to the waveguide modes coupled by the grating. In general, the number of guided modes allowed in a slab waveguide is proportional to the slab thickness. In our case, the wave-guiding slab, namely, the $\mu\text{c-Si:H}$ layer, is 4 times thicker than that in typical a-Si:H cells, which implies that the number of guided modes is increased by a factor of 4. In addition, the typical period that we used here ($P = 1.5\ \mu\text{m}$) is substantially longer than in the case of a-Si:H cells, which implies that numerous diffraction orders are generated by the periodic substrate in the wavelength range discussed here. As a consequence, it is rather complicated to analyze the origin of each peak in this system. However, as shown in Fig. 5, a number of fine peaks can be found in the absorption spectrum aside from the Fabry-Perrot interference fringes, whereas only the interference peaks are observable in the case of the flat cell. This result suggests that guided modes coupled via periodic textures also contribute to the EQE enhancement in our case. The discrepancy between the EQE and the absorption spectra in the long wavelength region originates from parasitic absorption in the inactive layers, such as free carrier absorption in the ITO and ZnO layers²⁶ and plasmonic absorption in the textured Ag layer.²⁷

J - V properties of the most efficient $\mu\text{c-Si:H}$ solar cells fabricated in this study are summarized in Table I. Compared with the flat cell, for the cell with the honeycomb texture, the efficiency of $\mu\text{c-Si:H}$ cells is boosted by more than 30%. Notably, the most efficient cells, as listed in the table, do not produce the maximum J_{SC} obtained in this study, even though the J_{SC} of these cells approach the maximum. In our case, the cell with (p)nc-SiO_x shows a slightly lower V_{OC} and FF, although the use of such wide gap materials is known to be advantageous for improving not only J_{SC} but

TABLE I. J - V parameters of $\mu\text{c-Si:H}$ cells fabricated on a flat and honeycomb textures with a period of $1.5\ \mu\text{m}$ and aspect ratio of ~ 0.23 . All the cells have an active area of $1\ \text{cm}^2$.

Substrate	p -layer	V_{OC} (V)	J_{SC} (mA/cm ²)	FF	Eff. (%)
Flat	$\mu\text{c-Si}$	0.539	17.5	0.742	7.0
Honeycomb	$\mu\text{c-Si}$	0.548	24.7	0.743	10.1
Honeycomb	nc-SiO _x	0.526	26.0	0.736	10.1

also V_{OC} and FF.⁵ This reveals that the efficiency can be further enhanced by improving the quality of (p)nc-SiO_x. In addition, J_{SC} improvement is also possible by applying higher transparency top transparent conducting oxide (TCO) layers such as In₂O₃:H²⁸ and n -layers.

To summarize, we have reported photocurrent and efficiency improvements in $1\text{-}\mu\text{m}$ -thick $\mu\text{c-Si:H}$ cells deposited on back reflectors with periodic honeycomb textures. The photocurrent enhancement is strongly dependent on the period and aspect ratio of the honeycomb textures. The highest photocurrent of $26.2\ \text{mA/cm}^2$ is obtained with a period of $1.5\ \mu\text{m}$ and an aspect ratio of > 0.2 . A series of the fine peaks observed in the absorption spectrum of the cell suggest that the waveguide modes, coupled via the honeycomb grating structure, play an important role in the absorption enhancement in the cell, although these peaks are not clearly observed in the EQE spectrum. It was also confirmed that the honeycomb textures are preferable for maintaining a high V_{OC} and FF. Accordingly, a high efficiency of 10.1% has been obtained in $1\text{-}\mu\text{m}$ -thick $\mu\text{c-Si:H}$ cells, indicating a high potential for periodic textures. The interplay between the cell thickness and the optimum texture parameters should be addressed in the future. Further, the application of our results to the superstrate configuration, which is a dominant architecture in current TFSSCs, also remains as a future task.

This work was supported by New Energy and Industrial Technology Development Organization (NEDO), Japan. Photolithography process was conducted at the AIST Nano-Processing Facility, supported by “Nanotechnology Network Japan” of the Ministry of Education, Culture, Sports, Science and Technology (MEXT), Japan.

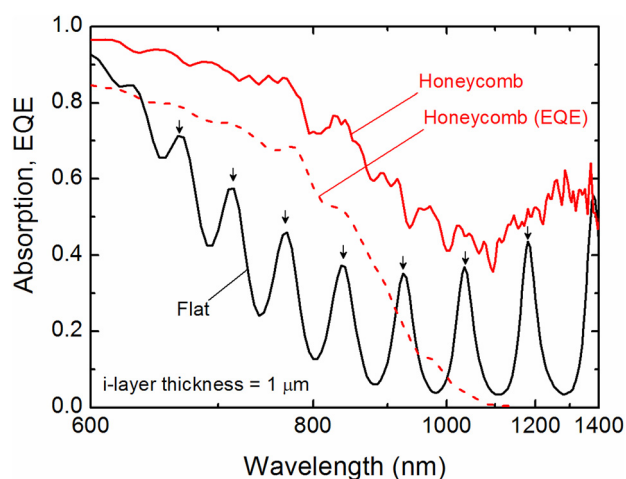


FIG. 5. Absorption spectra of the $\mu\text{c-Si:H}$ cells fabricated on a flat and the honeycomb substrate with $P = 1.5\ \mu\text{m}$. For the honeycomb substrate, the corresponding EQE spectrum is also plotted. Black arrows indicate the absorption peaks due to the Fabry-Perrot interference. The x axis is linearly proportional to the inverse of wavelength for better visibility.

- ¹J. Meier, S. Dubail, R. Platz, P. Torres, U. Kroll, J. A. Anna Selvan, N. Pellaton Vaucher, Ch. Hof, D. Fischer, H. Keppner, R. Flückiger, A. Shah, V. Shklover, and K.-D. Ufert, *Sol. Energy Mater. Sol. Cells* **49**, 35 (1997).
- ²K. Yamamoto, T. Suzuki, M. Yoshimi, and A. Nakajima, *Jpn. J. Appl. Phys., Part 2* **36**, L569 (1997).
- ³D. L. Staebler and C. R. Wronski, *J. Appl. Phys.* **51**, 3262 (1980).
- ⁴M. Kambe, A. Takahashi, N. Taneda, K. Masumo, T. Oyama, and K. Sato, in *Proc. 33rd IEEE Photovolt. Specialist Conf., San Diego* (2008), pp. 609–613.
- ⁵M. Despeisse, C. Battaglia, M. Boccard, G. Bugnon, M. Charrière, P. Cuony, S. Hänni, L. Löfgren, F. Meillaud, G. Parascandolo, T. Söderström, and C. Ballif, *Phys. Status Solidi A* **208**, 1863 (2011).
- ⁶M. Berginski, J. Hüpkens, M. Schulte, G. Schöpe, H. Steibig, B. Rech, and M. Wuttig, *J. Appl. Phys.* **101**, 074903 (2007).
- ⁷H. Sai, H. Jia, and M. Kondo, *J. Appl. Phys.* **108**, 044505 (2010).
- ⁸C. Battaglia, C.-M. Hsu, K. Söderström, J. Escarre, F.-J. Haug, M. Charrière, M. Boccard, M. Despeisse, D. T. L. Alexander, M. Cantoni, Y. Cui, and C. Ballif, *ACS Nano* **6**, 2790 (2012).
- ⁹K. Söderström, F.-J. Haug, J. Escarré, O. Cubero, and C. Ballif, *Appl. Phys. Lett.* **96**, 213508 (2010).
- ¹⁰F.-J. Haug, K. Söderström, A. Naqavi, and C. Ballif, *J. Appl. Phys.* **109**, 084516 (2011).

- ¹¹F.-J. Haug, A. Naqavi, and C. Ballif, *J. Appl. Phys.* **112**, 024516 (2012).
- ¹²O. Isabella, S. Solntsev, D. Caratelli, and M. Zeman, "3-D optical modeling of thin-film silicon solar cells on diffraction gratings," *Prog. Photovolt.* (to be published).
- ¹³F.-J. Haug, T. Söderström, M. Python, V. Terrazzoni-Daudrix, X. Niquille, and C. Ballif, *Sol. Energy Mater. Sol. Cells* **93**, 884 (2009).
- ¹⁴H. Sai and M. Kondo, *J. Appl. Phys.* **105**, 094511 (2009).
- ¹⁵M. Vanecek, O. Babchenko, A. Purkrt, J. Holovsky, N. Neykova, A. Poruba, Z. Remes, J. Meier, and U. Kroll, *Appl. Phys. Lett.* **98**, 163503 (2011).
- ¹⁶H. Sai, K. Saito, and M. Kondo, "Investigation of textured back reflectors with periodic honeycomb patterns in thin-film silicon solar cells for improved photovoltaic performance," *J. Photovolt.* (in press).
- ¹⁷H. Sai, Y. Kanamori, and M. Kondo, "Flattened light-scattering substrate and its application to thin-film silicon solar cells," *Jpn. J. Appl. Phys.* (in press).
- ¹⁸C. Haase and H. Stiebig, *Appl. Phys. Lett.* **91**, 061116 (2007).
- ¹⁹R. Dewan, V. Jovanov, C. Haase, H. Stiebig, and D. Knipp, *Appl. Phys. Express* **3**, 092301 (2010).
- ²⁰R. Dewan and D. Knipp, *J. Appl. Phys.* **106**, 074901 (2009).
- ²¹X. Sheng, J. Liu, I. Kozinsky, A. M. Agarwall, J. Michel, and L. C. Kimerling, *Adv. Mater.* **23**, 843 (2011).
- ²²Z. Yu, A. Raman, and S. Fan, *Opt. Express* **18**, A366 (2010).
- ²³S. E. Han and G. Chen, *Nano Lett.* **10**, 4692 (2010).
- ²⁴E. Yablonovitch, *J. Opt. Soc. Am. A* **72**, 899 (1982).
- ²⁵M. Python, O. Madani, D. Dominé, F. Meillaud, E. Vallat-Sauvain, and C. Ballif, *Sol. Energy Mater. Sol. Cells* **93**, 1714 (2009).
- ²⁶H. Fujiwara and M. Kondo, *Phys. Rev. B* **71**, 075109 (2005).
- ²⁷J. Springer, A. Poruda, L. Müllerova, M. Vanecek, O. Kluth, and B. Rech, *J. Appl. Phys.* **95**, 1427 (2004).
- ²⁸T. Koida, M. Kondo, K. Tsutsumi, A. Sakaguchi, M. Suzuki, and H. Fujiwara, *J. Appl. Phys.* **107**, 033514 (2010).